Suppression of discontinuous phase transitions by particle diffusion

Chul-Ung Woo,[1] Heiko Rieger,[2,3] and Jae Dong Noh[1]
[1]*Department of Physics, University of Seoul, Seoul 02504, Korea*
[2]*Department of Theoretical Physics & Center for Biophysics, Saarland University, 66123 Saarbrücken, Germany*
[3]*INM–Leibniz Institute for New Materials, Campus D2 2, 66123 Saarbrücken, Germany*

(Received 28 February 2022; accepted 4 May 2022; published 25 May 2022)

We investigate the phase transitions of the q-state Brownian Potts model in two dimensions (2D) comprising Potts spins that diffuse like Brownian particles and interact ferromagnetically with other spins within a fixed distance. With extensive Monte Carlo simulations we find a continuous phase transition from a paramagnetic to a ferromagnetic phase even for $q > 4$. This is in sharp contrast to the existence of a discontinuous phase transition in the equilibrium q-state Potts model in 2D with $q > 4$. We present detailed numerical evidence for a continuous phase transition and argue that diffusion generated dynamical positional disorder suppresses phase coexistence leading to a continuous transition.

DOI: 10.1103/PhysRevE.105.054144

I. INTRODUCTION

Phase transitions and critical phenomena have long been studied in statistical physics. Owing to advances in theoretical and numerical methods, equilibrium phase transitions are quite well understood. Microscopically different many-body models can have the same critical exponents characterizing the variation of certain physical properties near a critical point, thus representing the same universality class, which depend on but a few determinants like order parameter symmetry, spatial dimensionality, presence of quenched disorder, etc. [1]. Recently, nonequilibrium phase transitions attracted growing interest [2,3]. Broken detailed balance distinguishes nonequilibrium from equilibrium systems. As the detailed balance can be broken in many ways, nonequilibrium systems display a larger variety of phase transition scenarios.

A now paradigmatic example is active matter, which is characterized by energy consuming, self-propelled constituents and therefore driven out of equilibrium. Self-generated motility is responsible for various collective phenomena, like flocking, motility induced phase separation, active turbulence, etc. [4–6]. The seminal paper by Vicsek *et al.* [7] demonstrated that motility stabilizes long-range orientational order in two dimensions (2D), which would be unstable in the corresponding 2D equilibrium systems according to the Mermin-Wagner theorem [8]. Motility can also induce phase separation of active particles with repulsive interactions [9]. There are surging research activities to unveil the role of the motility in many-body systems [5,10–13].

Many studies of ensembles of self-propelled particles focus on the collective behavior of the spatial degrees of freedom such as the velocity and the position of particles. Motivated by collective effects that are induced by motility we focus in this paper on spins which are not fixed but move in space and search for an order-disorder phase transition. Concretely, we study the q-state Brownian Potts model in 2D, represented by Potts spins that diffuse like Brownian particles and interact ferromagnetically with other spins within a fixed distance. Whereas in the active Ising [10,11] or Potts [5,12,13] model the spin of a particle determines its direction of motion such that spin and spatial degrees of freedom are mutually coupled, we focus here on a unidirectional coupling: Particles diffuse *freely irrespective of spin states* while a spin interaction network evolves in time as particles diffuse. Even this simplified model displays interesting critical phenomena due to the ferromagnetic interactions.

The paper is organized as follows: In Sec. II, we introduce the q-state Brownian Potts model and discuss its features that are different from the equilibrium Potts model in 2D. In Sec. III we present our results of extensive Monte Carlo simulations, which show that the q-state Brownian Potts model has a continuous phase transition for all values of q, and determine the critical exponents. In Sec. IV we present an argument, based on a comparison of the timescales for particle diffusion and spin-spin correlation propagation, that diffusion impedes phase coexistence, which renders the transition continuous. We conclude the paper with summary and discussions in Sec. V.

II. q-STATE BROWNIAN POTTS MODEL

The model consists of $N = \rho L^d$ particles of density ρ on a square of area L^2 with periodic boundary conditions. The position of particle i is denoted as $\boldsymbol{r}_i \in \mathbb{R}^2$ and its Potts spin state by $\sigma_i \in \{1, \ldots, q\}$. The spins interact ferromagnetically with other particles j in a distance $|\mathbf{r}_j - \mathbf{r}_i| \leqslant r_0 \equiv 1$. We adopt parallel update dynamics in discrete time units: Given $\{\sigma_i(t), \boldsymbol{r}_i(t)\}$ at time step t, the spin states of all particles are updated according to the probability

$$P[\sigma_i(t+1) = \sigma] = \frac{1}{Z} \exp\left[K \sum_{j \in \mathcal{N}_i} \delta(\sigma, \sigma_j(t)) \right], \quad (1)$$

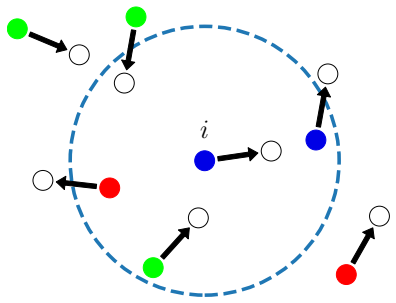

FIG. 1. Sketch illustrating the Brownian Potts model. The filled symbols represent the Brownian particles whose Potts spin states are color coded. Each particle interacts ferromagnetically with all particles within the distance r_0. The dashed circle denotes the interaction range of the particle i. After spin flips, particles perform a random jump of length v_0 to the position denoted by open symbols.

where $\delta(a, b)$ is the Kronecker-δ symbol, $\mathcal{N}_i$ denotes the set of particles within the distance r_0 from particle i, $K > 0$ the ferromagnetic spin-spin interaction strength, and Z is a normalization constant. Subsequently, each particle performs a jump of length v_0 in a random direction, $\boldsymbol{r}_i(t+1) = \boldsymbol{r}_i(t) + v_0(\cos\theta_i, \sin\theta_i)$, where $\theta_i \in (-\pi, \pi]$ are uniformly distributed independent random variables, generated anew in each time step (see Fig. 1). Note that the heat bath algorithm for the ferromagnetic q-state Potts model [14] has the same spin flip probability as in Eq. (1). Thus, when $v_0 = 0$, our model becomes the equilibrium q-state Potts model on a random lattice [15].

Particle diffusion introduces interesting features. It breaks the detailed balance and drives the system out of equilibrium. Since particles diffuse freely the system can be seen as being in contact with two thermal heat baths: a finite-temperature heat bath for the spin degrees of freedom with temperature $T \propto 1/K$ and an infinite temperature heat bath for the spatial degree of freedom. Nonequilibrium phase transitions of systems in thermal contact with two heat baths were investigated, for instance, in the context of the random q-neighbor Ising model [16,17].

Particle diffusion leads to particle density fluctuations, which acts like time-dependent disorder in the spin-spin interactions. Due to hopping, spin-spin interactions are spatially heterogeneous and each spin interacts with a fluctuating number of neighboring spins. Particle hoppings and spin flips occur simultaneously. Thus, the microscopic timescales for the particle hopping τ_p and for the spin flip τ_s are comparable. One can predict the consequence of the time-dependent disorder if the two timescales are well separated. For instance, in the limit $\tau_s/\tau_p \to 0$ or $v_0 \to 0$, the time-dependent disorder becomes quenched. There are rigorous results predicting the "rounding" of a discontinuous phase transition by quenched disorder for low-dimensional systems [18–21]. Thus, in the limit $v_0 \to 0$, we expect that our model belongs to the universality class of the Potts model with quenched disorder and undergoes a continuous phase transition at all values of q [22]. In the opposite limit, $\tau_s/\tau_p \to \infty$ or $v_0 \to \infty$, we expect that the mean-field theory is valid because spins are well mixed. The universality class of the transition in the intermediate case, $0 < v_0 < \infty$, remains elusive, which is what we intend to clarify in this paper. Since the two microscopic timescales are comparable, the macroscopic timescales at which particle density fluctuations and spin fluctuations propagate should be compared, which we will do in Sec. IV.

It is worth mentioning that the active Ising and the active Potts model introduced in Refs. [10–13]. In these models, particles with spin move on a 2D lattice and interact ferromagnetically with other particles on the same site. Their motion is biased toward a direction determined by their spin state. These models are discretized versions of the flocking model of Ref. [7]. Due to the bias and the ferromagnetic interaction, particles tend to move persistently together with neighboring particles, which stabilizes collective motion denoted as flocking. In contrast to the active Ising and Potts models, particles in the Brownian Potts model diffuse freely irrespective of the spin states. Thus, our model may be regarded as a passive Potts model.

III. NUMERICAL RESULTS

We have performed extensive Monte Carlo simulations for the Brownian Potts model with $q = 2, \ldots, 8$. Starting from a random initial state, Monte Carlo simulations are performed up to $T_{\max}$ time steps and a time series of the fraction n_σ of particles in the spin state σ $(= 1, \ldots, q)$ is obtained. The Potts order parameter [14], quantifying ferromagnetic order, is

$$m_s = \big(q \max_\sigma\{n_\sigma\} - 1\big)/(q-1). \tag{2}$$

Potts spin states can be represented by unit vectors $\{\boldsymbol{e}_\sigma\}$ in the $(q-1)$-dimensional space [14]. Using this representation, one can also define a vector order parameter

$$\boldsymbol{m}_v = \frac{1}{N}\sum_{i=1}^{N} \boldsymbol{e}_{\sigma_i} = \sum_\sigma n_\sigma \boldsymbol{e}_\sigma. \tag{3}$$

Using the time series $\{n_\sigma\}$, we can calculate the steady-state average of m_s and $|\boldsymbol{m}_v|$ and their moments and probability distributions. Both quantities display a qualitatively similar behavior. We investigate the phase transition by varying the coupling strength K with fixed interaction range $r_0 = 1$, hopping length $v_0 = 1/2$, and particle density $\rho = 1$. We also performed simulations for $\rho = 2$ and 4 and reached the same conclusion. Thus we only present the numerical results at $\rho = 1$. The largest system size we considered is $L = 512$ with $T_{\max} = 4 \times 10^8$, which is sufficiently long to reach a steady state. Data in the time interval from $T_{\max}/10$ to $T_{\max}$ steps are used for the steady-state average. In order to estimate the statistical uncertainty of the numerical results, we used the bootstrap or resampling method [23]: Given a steady-state time series $\{n_\sigma\}$, we resample S subsets each of which consists of randomly chosen $T_{\max}/S$ data points. A statistical error of a quantity is measured by the standard deviation of S sampled averages. We chose $S = 100$.

Figure 2 shows the order parameter $m = \langle|\boldsymbol{m}_v|\rangle$ and the Binder cumulant $U_4 \equiv 1 - \langle|\boldsymbol{m}_v|^4\rangle/(3\langle|\boldsymbol{m}_v|^2\rangle^2)$ for $q = 3$ and 6. The order parameter shows that the system has a phase transition from a paramagnetic to a ferromagnetic phase. When K is smaller than a critical value K_c, the order parameter decays to zero as L increases. On the other hand, when $K > K_c$, it converges to a finite value. The critical interaction strength

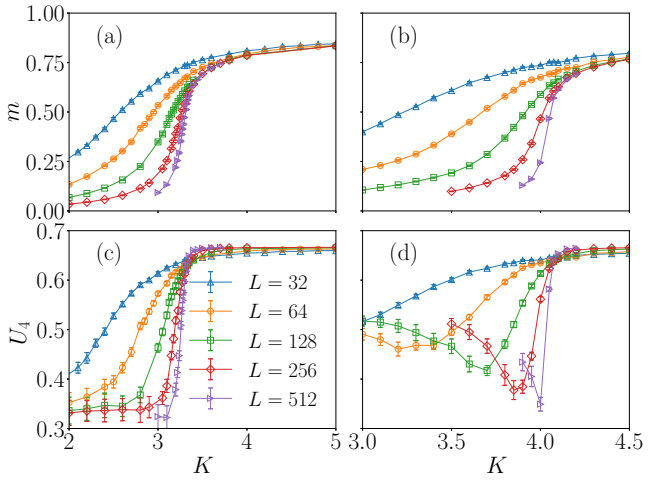

FIG. 2. Order parameter (top) and the Binder cumulant (bottom) of the Brownian Potts model for $q = 3$ [(a) and (c)] and $q = 6$ [(b) and (d)].

K_c can be estimated from the intersection of the curves of the Binder cumulants U_4 for different system sizes [see Figs. 2(c) and 2(d)]. We obtain $K_c(q = 3) = 3.33(3)$ and $K_c(q = 6) = 4.08(3)$. We will discuss the critical exponents below.

A. Order of the transition

The Binder cumulant U_4 shown in Figs. 2(c) and 2(d) has a dip in the paramagnetic phase. The dip becomes more pronounced at larger values of q. The Binder cumulant diverges (to $-\infty$) at a discontinuous phase transition point [24]. Recalling that the equilibrium Potts model in 2D has a discontinuous phase transition for $q > 4$, we need to examine whether the dip is an indication of the discontinuous phase transition.

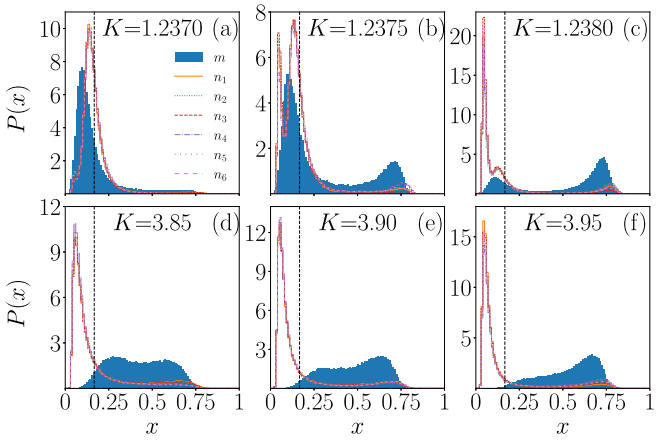

FIG. 3. Histograms of the order parameter $x = |\boldsymbol{m}_v|$ (blue, filled curves) and spin fractions $x = n_\sigma$ with $\sigma = 1, 2, \ldots, q$ (solid lines). Top row [(a), (b), and (c)] shows the histograms for the equilibrium Potts model and the bottom row [(d), (e), and (f)] for the Brownian Potts model. Data are for $q = 6$, $L = 128$, and $K \simeq K_c$. Note that $K_c = \ln(1 + \sqrt{6}) \simeq 1.2382$ for the equilibrium six-state Potts model and $K_c \sim 4.08(3)$ for the Brownian Potts model. The dotted vertical lines indicate the value $x = 1/q$.

In Fig. 3, we compare the order parameter histograms of the equilibrium Potts model and the Brownian Potts model with $q = 6$. The equilibrium Potts model displays a behavior characteristic for a discontinuous phase transition: The histogram has a single peak corresponding to a paramagnetic phase at small K [Fig. 3(a)], double peaks indicating phase coexistence [Fig. 3(b)] for intermediate values of K, and a single peak corresponding to a ferromagnetic phase at large K [Fig. 3(c)]. The order parameter histogram for the Brownian Potts model also has double peaks, but they are much less pronounced than those observed in the equilibrium model.

The order parameter histograms, $P(|\boldsymbol{m}_v|)$, alone do not provide a conclusive evidence for phase coexistence. Thus, we further investigate the histograms, $P(n_\sigma)$, of the fraction n_σ of particles in the spin state σ $(= 1, \ldots, q)$. In the disordered paramagnetic phase, all spin states are equally populated with statistical fluctuations. Namely, all histograms of n_σ should have a peak around $x = 1/q$. In the ordered ferromagnetic phase, one spin state, say, σ_m, dominates. Thus, the histogram of n_{σ_m} should have a peak at $x > 1/q$ while the other $(q - 1)$ histograms at $x < 1/q$. In Fig. 3(b) for the equilibrium Potts model, we find the peaks corresponding to both phases. The central peak at $x \simeq 1/q$ corresponds to the disordered phase, which is well separated from the other two peaks corresponding to the ordered phase. Our simulation time $T_{\max}$ is so long that the system alternates between the disordered state and the ordered states with different σ_m. This three-peak structure is an evidence for phase coexistence in the equilibrium six-state Potts model.

On the other hand, the histograms of n_σ for the Brownian Potts model do not have a peak at $x \simeq 1/q$ representing the paramagnetic phase [see Figs. 3(d), 3(e) and 3(f)]. This is a clear and decisive evidence for the absence of phase coexistence. We also performed the same analysis for other values of $q = 2, \ldots, 8$, which lead to the same conclusion that the Brownian Potts model has a continuous phase transition irrespective of the value q. We will substantiate this conclusion with a theoretical argument later.

The apparent double peaks in the order parameter histogram is attributed to the discrete symmetry of the Potts spin. The Potts order parameter $\boldsymbol{m}_v$ lies within a $(q - 1)$-dimensional polyhedron [14]. For instance, it lies inside an equilateral triangle for $q = 3$. As the coupling constant approaches K_c from below, the order parameter deviates from the center of the polyhedron and moves toward a vertex developing a peak in the order parameter histogram. Due to fluctuations at finite L, it does not stay near a single vertex but keeps diffusing to the other vertices. In the transient period, the order parameter magnitude shrinks because it is limited by the faces of the polyhedron. This effect can result in an additional bump in the order parameter histogram. The broad double peaks observed in Figs. 3(d) and 3(e) and the apparent dips in the Binder cumulant shown in Fig. 2(d) are plausibly a consequence of this effect.

We also confirmed numerically that the equilibrium $(q = 3)$-state Potts model in 2D has a similar bump in the order parameter histogram and a dip in the Binder parameter. The equilibrium three-state Potts model is known to have a continuous phase transition. Therefore, the unusual behavior of the order parameter histogram and the Binder parameter

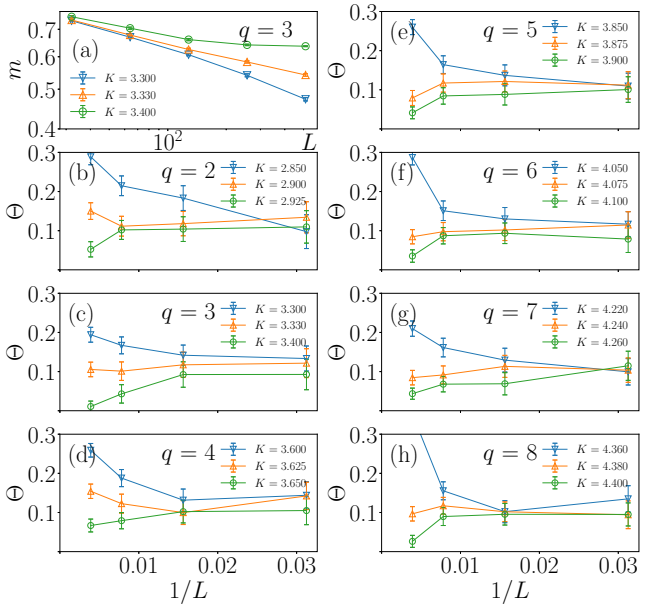

FIG. 4. (a) Order parameter of the Brownian Potts model as function of L for $q = 3$ at different coupling constants K. [(b)–(h)] Effective exponent Θ as a function of $1/L$ near the critical points for different values of q.

should not be taken as an evidence for a discontinuous phase transition.

B. Critical scaling of the order parameter

After establishing that the phase transitions are continuous ones, we will estimate the critical exponents via finite-size scaling. Near the critical point, the order parameter is assumed to have the scaling form

$$m(K, L) = L^{-\beta/\nu} F_m(tL^{1/\nu}), \tag{4}$$

where $t \equiv (K - K_c)/K_c$ is the reduced coupling strength (akin to a reduced temperature), ν is the correlation length exponent describing the divergence of the correlation length $\xi \sim |t|^{-\nu}$, β is the order parameter exponent, and $F_m(x)$ is a scaling function. At the critical point, the order parameter follows the power law $m(K_c, L) \sim L^{-\beta/\nu}$. The exponent β/ν can be estimated from the effective exponent $\Theta(K, L) \equiv -\log[m(K, 2L)/m(K, L)]/\log 2$. It converges to β/ν at $K = K_c$ and crosses over to the trivial value 0 for $K > K_c$ and $d/2$ for $K < K_c$. Figure 4(a) demonstrates the power-law scaling at the critical point and the crossover in the off-critical regime. In Figs. 4(b)–4(h), we present the effective exponent Θ as a function of $1/L$ near critical points at $q = 2, \ldots, 8$. An overall curvature in the plot Θ vs. $1/L$ indicates a deviation from the critical point, which allows us to estimate the critical point and the exponent β/ν and their numerical uncertainty. They are summarized in Table I. The exponent β/ν falls within the range $\beta/\nu = 0.10 \pm 0.05$ for all values of $2 \leqslant q \leqslant 8$. From our data with $L \leqslant 512$, it is hard to draw a conclusion whether the exponent has a q dependence.

In addition to the order parameter, we also calculated the order parameter fluctuation $\chi \equiv N(\langle|\boldsymbol{m}_v|^2\rangle - \langle|\boldsymbol{m}_v|\rangle^2)$. Analogously to the magnetic susceptibility in the equilibrium system, it is expected to follow the finite-size scaling form,

$$\chi(K, L) = L^{\gamma/\nu} F_\chi(tL^{1/\nu}), \tag{5}$$

where the exponent γ characterize the power-law scaling of $\chi \sim |t|^{-\gamma}$ and F_χ is a scaling function. We have performed the data collapse analyses of m and χ using the scaling forms in Eqs. (4) and (5) to determine the critical exponents $1/\nu$ and γ/ν. Our estimates of the critical coupling constants and the critical exponents at all values of q are summarized in Table I. Figure 5 shows the scaling plots at $q = 5$ and 7. One observes that χ suffers from strong finite-size effects.

Particles in the active Ising model [11] become passive if one turns off the spin-dependent hopping bias. The phase transition in that limit belongs to the universality class of the 2D equilibrium Ising model [11]. Our result for β/ν is comparable with $(\beta/\nu) = 1/8, 2/15$ and $1/8$ of the lattice q-state Potts model with $q = 2$, 3, and 4, respectively, within the numerical uncertainty. It may suggest that the Brownian Potts model belong to the same universality class of the equilibrium Potts model. However, the continuous phase transition in the Brownian Potts model for $q > 4$ excludes such a possibility. The numerical results for $1/\nu$ at $q = 3$ and 4 are

TABLE I. Critical interaction strength and the exponents.

q	K_c	β/ν	$1/\nu$	γ/ν	Z_R
2	2.90(5)	0.10(5)	1.00(10)	1.70(20)	2.15(10)
3	3.33(3)	0.10(5)	1.03(10)	1.75(20)	2.25(10)
4	3.63(3)	0.10(5)	1.05(10)	1.80(20)	2.35(10)
5	3.87(5)	0.10(5)	1.08(10)	1.85(20)	2.35(10)
6	4.08(3)	0.10(5)	1.10(10)	1.90(20)	2.38(10)
7	4.24(3)	0.09(5)	1.13(10)	1.95(20)	2.40(10)
8	4.38(3)	0.09(5)	1.15(10)	1.95(30)	2.45(10)

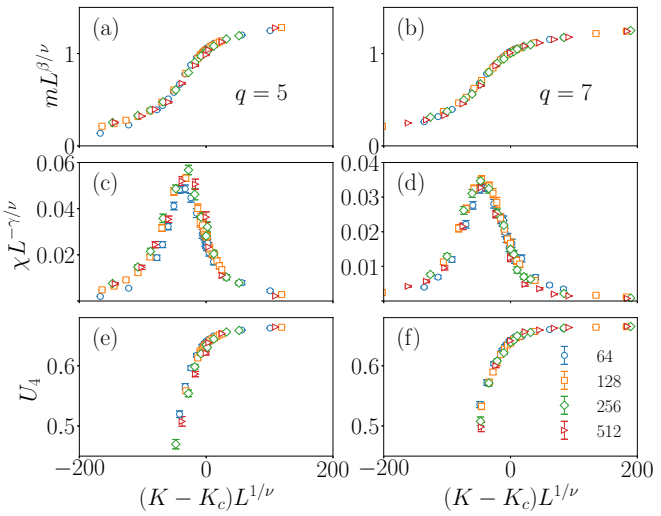

FIG. 5. Scaling plots of m, χ, and U_4 at $q = 5$ in (a), (c), and (e) and at $q = 7$ in (b), (d), and (f) using the numerical estimates listed in Table I.

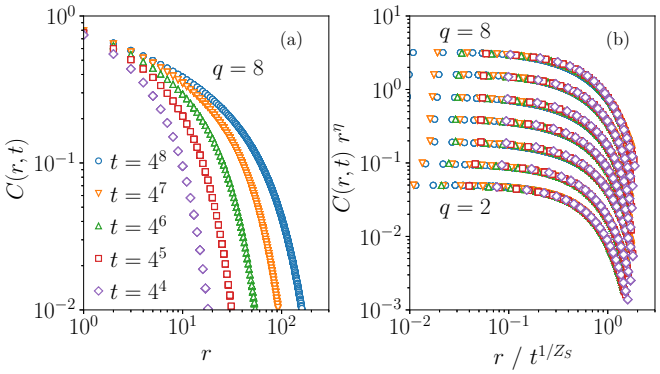

FIG. 6. (a) Spin-spin correlation function at $t = 4^4, \ldots, 4^8$ evaluated at the critical point for $q = 8$. Data points are aligned along a single curve, which indicates that the correlation function is isotropic. (b) Scaling plots according to Eq. (7) at all values of $2 \leqslant q \leqslant 8$. For a better visualization, we shift the data sets vertically by multiplying 2^{q-6}. All the data are obtained from the ensemble average over 100 samples. The system size is $L = 4096$.

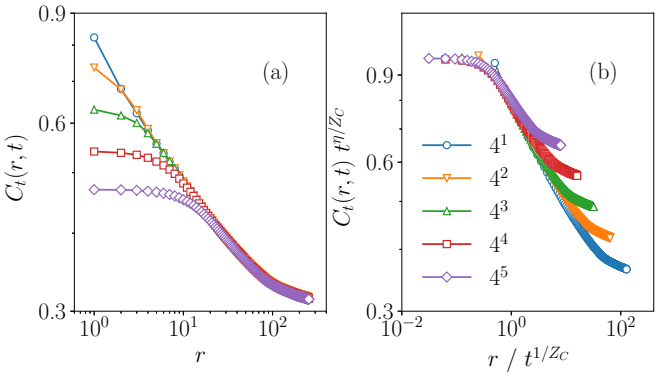

FIG. 7. (a) Two-time correlation functions at $t = 4^1, \ldots, 4^5$ evaluated at the critical point for $q = 3$ and $L = 512$ averaged over 100 samples. (b) Scaling plot according to Eq. (9) with the correlation time exponent $Z_C = 2.0$ and $\eta = 0.21$.

not consistent with those of the equilibrium 2D Potts model [$1/\nu = 6/5$ ($q = 3$) and $3/2$ ($q = 4$)] either [14].

IV. TIMESCALES AND NATURE OF THE TRANSITION

Density fluctuations due to diffusion render a particle-particle interaction network inhomogeneous. Particles in a dense (dilute) region have more (fewer) neighbors. Moreover, the interaction network evolves in time as particles diffuse. In order to gain an insight on the influence of the time-dependent disorder on the phase transition, we compare timescales for relevant degrees of freedom.

Obviously, there is a *diffusion timescale* $\tau_D \sim \xi^{Z_D}$ with $Z_D = 2$ characterizing the particle diffusion over the distance ξ. In addition, there is a *relaxation timescale* τ_R which it takes for the spins to reach the steady state. We characterize the scaling behavior of τ_R from the *equal-time* spin-spin correlation function. For the correlation function of the off-lattice system, we divide the two-dimensional plane into L^2 unit cells $\{\alpha = 1, \ldots, L^2\}$ and define a cell spin $\boldsymbol{S}(\boldsymbol{r}_\alpha, t) = \sum_{\boldsymbol{r}_i \in \alpha} \boldsymbol{e}_{\sigma_i}$ as the sum of spins of particles in a cell located at $\boldsymbol{r}_\alpha \in \mathbb{Z}^2$ at time t. The equal-time correlation function is then defined as

$$C_e(\boldsymbol{r}, t) = \frac{1}{L^2} \sum_{\alpha} \langle \boldsymbol{S}(\boldsymbol{r}_\alpha, t) \cdot \boldsymbol{S}(\boldsymbol{r}_\alpha + \boldsymbol{r}, t) \rangle \tag{6}$$

with a random initial state at $t = 0$. Figure 6(a) shows the correlation function, $C_e(\boldsymbol{r}, t)$, for $q = 8$, $L = 4096$, and $K = K_c$. It decays algebraically with an exponent η for small r and exponentially for large r. The crossover defines the length-scale-dependent relaxation time τ_R, which turns out to follow a power law $\tau_R \sim \xi^{Z_R}$ with the relaxation time exponent Z_R. Figure 6(b) shows that the correlation functions satisfy the scaling form

$$C_e(\boldsymbol{r}, t) = r^{-\eta} F_e(r/t^{1/Z_R}) \tag{7}$$

with Z_R given in Table I. The correlation function exponent η takes the value around 0.25 at all values of q.

The relaxation time exponent Z_R characterizes the growth of the correlation length $\xi \sim t^{1/Z_R}$ in the transient regime. It is noteworthy that $Z_R > Z_D$ for all q. The particle diffusion is a faster process than the spin ordering dynamics. This result implies that the diffusion-induced spatial heterogeneity is substantially different from quenched (time-independent) disorder. Quenched disorder is known to suppress a discontinuous phase transition [19–21]. For instance, the disordered equilibrium q-state Potts model in 2D has a continuous phase transition at all values of q [22]. The fact that $Z_R > Z_D$ provokes the question for the mechanism leading to the suppression of the discontinuous phase transition in the Brownian Potts model with time-dependent diffusion-induced disorder, which will be addressed shortly.

The correlation time in the steady state can be characterized by the *two-time* correlation function

$$C_t(\boldsymbol{r}, t) = \frac{1}{L^2} \sum_{\alpha} \langle \boldsymbol{S}(\boldsymbol{r}_\alpha, t_0) \cdot \boldsymbol{S}(\boldsymbol{r}_\alpha + \boldsymbol{r}, t_0 + t) \rangle \tag{8}$$

with $t_0 \gg L^{Z_R}$. The spatial correlation decays as the steady-state fluctuation spreads. This dynamic critical behavior is captured by the dynamic scaling form

$$C_t(\boldsymbol{r}, t) = t^{-\eta/Z_C} F_t(r/t^{1/Z_C}) \tag{9}$$

with the correlation time exponent Z_C characterizing the correlation timescale $\tau_C \sim \xi^{Z_C}$ over a distance ξ.

The numerical data for the critical two-point correlation function C_t for $q = 3$ and $L = 512$ are presented in Fig. 7 [25]. Our data for C_t show a good data collapse according to the scaling form (9) with an exponent $Z_C \simeq 2.0$. This value is close to the dynamic exponent Z_D of diffusion. We expect that Z_C is equal to Z_D for all values of q because diffusion is the dominant mechanism that propagates fluctuations.

Interestingly, the nonstationary relaxation time and the stationary correlation timescale differently with $Z_R > Z_C \simeq Z_D$. This observation indicates a potential reason for the absence of phase coexistence in the Brownian Potts model. To elaborate we propose a thought experiment that consists of introducing a ferromagnetic domain into the system in the steady state at $K = K_c$ (see Fig. 8). The system is then driven away from the steady state locally. Across the domain

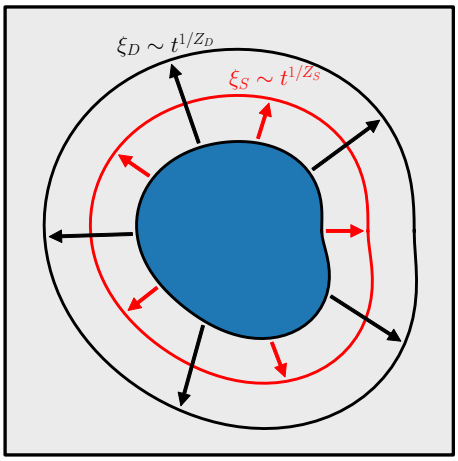

FIG. 8. Ferromagnetic domain (filled blue area) inside a steady-state background. The length scales associated with particle diffusion and spin ordering are represented with the black and red arrows, respectively.

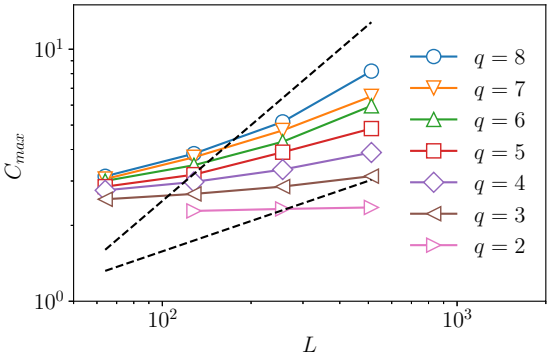

FIG. 9. Log-log plots for the peak values of the specific heat. At $q = 2$, $C_{\max} \sim \ln L$. On the other hand, the curvature for $q > 3$ indicates a crossover to a power-law scaling. For comparison, dashed straight lines with slope $2/5$ and 1 are shown, which are representative for the equilibrium Potts model with $q = 3$ and 4, respectively.

boundary, ordered spins diffuse into the bulk, in time t by a distance of $\xi_D \sim t^{1/Z_D}$. On the other hand, spin-order propagates in this time only a distance $\xi_R \sim t^{1/Z_R} \ll \xi_D$ from the boundary. Thus, the diffusing particles are absorbed into the disordered bulk and the initially ordered domain keeps shrinking and vanishes eventually. This argument indicates that particle diffusion destabilizes phase coexistence as long as $Z_R > Z_D$. It provides a self-consistent explanation why the Brownian Potts model exhibits a continuous phase transition without phase coexistence. We can phrase the same argument in terms of the correlation length $\xi_C \sim t^{1/Z_C}$: with $Z_C \simeq Z_D < Z_R$, the propagation of critical fluctuations dominates the domain growth dynamics and sweep away ordered domains.

V. SUMMARY AND DISCUSSIONS

We have investigated the influence of passive diffusion on the order-disorder phase transition and the critical behavior in the Brownian q-state Potts model in two dimensions. Particle diffusion introduces interesting aspects that are absent in the equilibrium counterpart of immobile spins on a lattice: (i) It breaks detailed balance and drives the system out of equilibrium. A weak breaking of detailed balance is irrelevant for some systems. [26,27]. In the Brownian Potts model particle diffusion turns out to be strong in the sense that it changes the nature of the transition at least for $q > 4$. (ii) The particle diffusion introduces time-dependent disorder in the spin-spin interaction network. At the critical point, we find that density and spin fluctuations are faster processes than the ordering dynamics $Z_R > Z_D \simeq Z_C$. Thus, the diffusion-induced time-dependent disorder is substantially different from quenched disorder. We argued that time-dependent disorder suppresses phase coexistence, which is consistent with our numerical results that the Brownian Potts model displays a continuous phase transition.

We remark that quenched disorder also suppresses the discontinuity of the phase transition [19]. The 2D random-bond Potts models indeed undergo a continuous phase transition at any values of q [22,28]. The correlation length exponent is almost constant $\nu \simeq 1.0$ and the correlation function displays a multiscaling behavior. It is interesting to note that the correlation length exponent of the Brownian Potts model also has a weak dependence on q. On the other hand, we do not find any evidence for the multiscaling behavior in the Brownian Potts model.

The histograms, shown in Fig. 3, are the evidence for the absence of phase coexistence in the Brownian Potts model even for $q > 4$. However, the universality class for the Brownian Potts model remains still elusive. Although the critical exponents summarized in Table I vary slightly with q, the numerical uncertainty is too large to draw a final conclusion regarding the universality class. We also defined an energy-like quantity $E = -\frac{1}{2}\sum_{|\boldsymbol{r}_i - \boldsymbol{r}_j| < r_0} \delta(\sigma_i, \sigma_j)$ and measured its second moment $C \equiv (\langle E^2 \rangle - \langle E \rangle^2)/L^2$ as an analogy to the specific heat of the equilibrium Potts model. Near $K = K_c$, it has a peak whose height increases as L. We present the peak values in Fig. 9. For $q = 2$, it increases logarithmically with the system size L, which is a characteristics of the Ising universality class. The data for $q \geqslant 3$ deviate from the logarithmic scaling. The crossover indicates a q-dependent critical behavior. The curvature in the plot, however, indicates that the asymptotic behavior can be accessed in much larger systems.

In the Brownian Potts model, particles interact on a time-dependent disordered network whose edges correspond to particle pairs that have a distance $r \leqslant r_0$. Remarkably, these instantaneous interaction networks do not percolate for the particle density $\rho = 1$ and $r_0 = 1$ considered here, which means that they do not contain a single infinite cluster but comprise only finite clusters of an average size. This can be seen by recurring to random plane networks [29], which are defined by overlapping objects of size a distributed randomly in the plane with density ρ. For disks it is known that those networks percolate for $\rho \cdot a \geqslant 1.127$ [30,31], which implies that for $\rho = 1$ the disk radius must be larger than $r_c = 0.599$. For our instantaneous interaction network this means that the particle-particle interaction range r_0 should be larger than $2r_c = 1.197$ in order to form percolating interaction clusters, which is not the case here. If the interaction network would be static, i.e., the particle would be

immobile, long-range order could not emerge on the basis of only finite interaction clusters. On the other hand, in the Brownian Potts model long-range order emerges in spite of the nonpercolating instantaneous interaction networks: Particle diffusion propagates spin order with time beyond the instantaneous interaction clusters and thus generates an effective, time-averaged global connectivity of the interaction network. If the particle density is smaller than a certain threshold value ρ_c, the interaction network fails to maintain a global connectivity and long-range order ceases to exist for any coupling constant. For the Ising case with $q = 2$, we numerically found that this threshold density is given by $\rho_c \simeq 0.93$. It would be interesting to study the nature of the dynamical percolation transition, which we leave for a future study.

The coupling between the spin and spatial degrees of freedom turns out to be an important aspect determining the nature of phase transitions. The Brownian Potts model has a unidirectional coupling: Particles diffuse freely irrespective of spin states, but the particle diffusion modifies the interaction network of spins. It would be interesting to study the order-disorder transition and the flocking transition in a system with a coupling in both directions. There were a few studies along this line [32,33]. We hope that our work triggers further systematic analysis of the phase transitions and the critical phenomena in passively or actively moving spin systems.

ACKNOWLEDGMENTS

This work is supported by the National Research Foundation of Korea (KRF) grant funded by the Korea government (MSIP) (Grant No. 2019R1A2C1009628). We acknowledge the computing resources of Urban Big data and AI Institute (UBAI) at the University of Seoul.

[1] H. E. Stanley, Scaling, universality, and renormalization: Three pillars of modern critical phenomena, Rev. Mod. Phys. **71**, S358 (1999).

[2] H. Hinrichsen, Non-equilibrium critical phenomena and phase transitions into absorbing states, Adv. Phys. **49**, 815 (2000).

[3] R. Wittkowski, A. Tiribocchi, J. Stenhammar, R. J. Allen, D. Marenduzzo, and M. E. Cates, Scalar ϕ^4 field theory for active-particle phase separation, Nat. Commun. **5**, 4351 (2014).

[4] S. Ramaswamy, Active matter, J. Stat. Mech.: Theory Exp. (2017) 054002.

[5] M. R. Shaebani, A. Wysocki, R. G. Winkler, G. Gompper, and H. Rieger, Computational models for active matter, Nat. Rev. Phys. **2**, 181 (2020).

[6] J. O'Byrne, Y. Kafri, J. Tailleur, and F. v. Wijland, Time irreversibility in active matter, from micro to macro, Nat. Rev. Phys. **4**, 167 (2022).

[7] T. Vicsek, A. Czirók, E. Ben-Jacob, I. Cohen, and O. Shochet, Novel Type of Phase Transition in a System of Self-Driven Particles, Phys. Rev. Lett. **75**, 1226 (1995).

[8] N. Goldenfeld, *Lectures on Phase Transitions and the Renormalization Group* (Addison-Wesley, Boston, MA, 1992).

[9] M. E. Cates and J. Tailleur, Motility-induced phase separation, Annu. Rev. Condens. Matter Phys. **6**, 219 (2015).

[10] A. P. Solon and J. Tailleur, Revisiting the Flocking Transition Using Active Spins, Phys. Rev. Lett. **111**, 078101 (2013).

[11] A. P. Solon and J. Tailleur, Flocking with discrete symmetry: The two-dimensional active Ising model, Phys. Rev. E **92**, 042119 (2015).

[12] S. Chatterjee, M. Mangeat, R. Paul, and H. Rieger, Flocking and reorientation transition in the 4-state active Potts model, Europhys. Lett. **130**, 66001 (2020).

[13] M. Mangeat, S. Chatterjee, R. Paul, and H. Rieger, Flocking with a q-fold discrete symmetry: Band-to-lane transition in the active Potts model, Phys. Rev. E **102**, 042601 (2020).

[14] F. Y. Wu, The Potts model, Rev. Mod. Phys. **54**, 235 (1982).

[15] Since we adopt the parallel update rule, the spins relax into a thermal equilibrium state associated with a Hamiltonian that is slightly modified from the conventional Potts model Hamiltonian.

[16] J.-M. Park and J. D. Noh, Tricritical behavior of nonequilibrium Ising spins in fluctuating environments, Phys. Rev. E **95**, 042106 (2017).

[17] A. Jędrzejewski, A. Chmiel, and K. Sznajd-Weron, Oscillating hysteresis in the q-neighbor Ising model, Phys. Rev. E **92**, 052105 (2015).

[18] Y. Imry and S.-k. Ma, Random-Field Instability of the Ordered State of Continuous Symmetry, Phys. Rev. Lett. **35**, 1399 (1975).

[19] R. L. Greenblatt, M. Aizenman, and J. L. Lebowitz, On spin systems with quenched randomness: Classical and quantum, Physica A **389**, 2902 (2010).

[20] M. Aizenman and J. Wehr, Rounding of First-Order Phase Transitions in Systems with Quenched Disorder, Phys. Rev. Lett. **62**, 2503 (1989).

[21] K. Hui and A. N. Berker, Random-Field Mechanism in Random-Bond Multicritical Systems, Phys. Rev. Lett. **62**, 2507 (1989).

[22] T. Olson and A. P. Young, Monte Carlo study of the critical behavior of random bond Potts models, Phys. Rev. B **60**, 3428 (1999).

[23] M. Newman and G. T. Barkema, *Monte Carlo Methods in Statistical Physics* (Oxford University Press, New York, 1999).

[24] K. Binder and D. W. Heermann, *Monte Carlo Simulation in Statistical Physics, An Introduction*, Springer Series in Solid-State Sciences, Vol. 80 (Springer-Verlag, Berlin, 2010).

[25] The calculation of the two-time correlation function is computationally demanding since it requires an ensemble average over a large number of samples (100 samples in the present work) in the steady state (i.e., $t_0 \gg L^{Z_R}$), for which reason we restrict ourselves here to $q = 3$ and $L \leqslant 512$. On the other hand, it is relatively easier to obtain the ensemble-averaged equal-time correlation function shown in Fig. 6 since it is measured in the transient regime.

[26] G. Grinstein, C. Jayaprakash, and Y. He, Statistical Mechanics of Probabilistic Cellular Automata, Phys. Rev. Lett. **55**, 2527 (1985).

[27] U. C. Täuber, V. K. Akkineni, and J. E. Santos, Effects of Violating Detailed Balance on Critical Dynamics, Phys. Rev. Lett. **88**, 045702 (2002).

[28] J. Cardy and J. L. Jacobsen, Critical Behavior of Random-Bond Potts Models, Phys. Rev. Lett. **79**, 4063 (1997).

[29] E. N. Gilbert, Random plane networks, J. Soc. Industr. Appl. Math. **9**, 533 (1961).

[30] P. Balister, B. Bollobás, and M. Walters, Continuum percolation with steps in the square or the disc, Random Struct. Alg. **26**, 392 (2005).

[31] S. Mertens and C. Moore, Continuum percolation thresholds in two dimensions, Phys. Rev. E **86**, 061109 (2012).

[32] K. P. O'Keeffe, H. Hong, and S. H. Strogatz, Oscillators that sync and swarm, Nat. Commun. **8**, 1504 (2017).

[33] H. K. Lee, K. Yeo, and H. Hong, Collective steady-state patterns of swarmalators with finite-cutoff interaction distance, Chaos **31**, 033134 (2021).